

# **Polarization-interferometry-based wavelength-interrogation surface plasmon resonance imager for analysis of microarrays**

Zhiyi Liu  
Le Liu  
Xiaoxiao Wang  
Heng Shi  
Xinyuan Chong  
Suihua Ma  
Yanhong Ji  
Jihua Guo  
Hui Ma  
Yonghong He

# Polarization-interferometry-based wavelength-interrogation surface plasmon resonance imager for analysis of microarrays

Zhiyi Liu,<sup>a</sup> Le Liu,<sup>b</sup> Xiaoxiao Wang,<sup>c</sup> Heng Shi,<sup>a</sup> Xinyuan Chong,<sup>a</sup> Suihua Ma,<sup>a</sup> Yanhong Ji,<sup>d</sup> Jihua Guo,<sup>a</sup> Hui Ma,<sup>a</sup> and Yonghong He<sup>a</sup>

<sup>a</sup>Tsinghua University, Graduate School at Shenzhen, Laboratory of Optical Imaging and Sensing, Shenzhen, 518055, China

<sup>b</sup>Tsinghua University, Graduate School at Shenzhen, Laboratory of Advanced Power Source, Shenzhen, 518055, China

<sup>c</sup>Tsinghua University, School of Life Science, Beijing, 100084, China

<sup>d</sup>South China Normal University, MOE Key laboratory of Laser Life Science & Institute of Laser Life Science, Guangzhou, 510631, China

**Abstract.** Polarization interferometry (PI) techniques, which are able to improve surface plasmon resonance (SPR) sensing performance and reduce restrictions on allowable parameters of SPR-supporting metal films, have been experimentally realized only in SPR sensors using monochromatic light as a source. Wavelength-interrogation SPR sensors modulated by PI techniques have not been reported due to the wavelength-sensitive characterization of PI phase compensators. In this work we develop a specially designed rhombic prism for phase compensating which is totally insensitive to wavelength. For the first time we successfully apply PI technique to a wavelength-interrogation SPR imager. This imager is able to offer two-dimensional imaging of the whole array plane. As a result of PI modulation, resolutions of  $1.3 \times 10^{-6}$  refractive index unit (RIU) under the normal condition and  $3.9 \times 10^{-7}$  RIU under a more time-consuming condition are acquired. The application of this imager was demonstrated by reading microarrays for identification of bacteria, and SPR results were confirmed by means of fluorescence imaging. © 2012 Society of Photo-Optical Instrumentation Engineers (SPIE). [DOI: 10.1117/1.JBO.17.3.036002]

Keywords: surface plasmon resonance; surface plasmon resonance imager; polarization interferometry; microarray.

Paper 11227 received May 8, 2011; revised manuscript received Jan. 3, 2012; accepted for publication Jan. 6, 2012; published online Mar. 12, 2012.

## 1 Introduction

Microarray technology, which facilitates sensing of multiple biomolecular interactions in parallel, has revolutionized the biomedical research since its advent in the end of the 20th century.<sup>1,2</sup> A well-known approach to microarray analysis in a label-free and real-time manner is the surface plasmon resonance (SPR) method.<sup>3,4</sup> There are three main configurations used in SPR sensors: amplitude measurement, phase modulation, and spectroscopy-based measurement.<sup>5</sup> Amplitude measurements are based on a relationship between the change in reflective light intensity and the refractive index of bound analyte.<sup>6</sup> Because they are based on direct intensity variations, amplitude measurements are vulnerable to stray light and spatial inhomogeneity in the light source.<sup>7</sup> SPR sensors based on phase modulation make use of the phase shift when SPR occurs.<sup>8,9</sup> Although these sensors have exhibited high sensitivity, they suffer from the instability of the complicated setup and the limited dynamic range.<sup>10</sup> Spectroscopy-based measurements include two modes: wavelength interrogation and angular interrogation. They measure the reflectivity as a function of the incident angle (angular mode) or wavelength (wavelength mode). Owing to the acquisition of the complete resonance curve, spectroscopy-based measurements offer better signal-to-noise ratio compared

with the other configurations.<sup>7</sup> During the past years, some wavelength-interrogation SPR sensors have been described in the literature.<sup>7,11–13</sup> Yuk et al. proposed a wavelength interrogation-based SPR biosensor for analysis of protein interactions on protein arrays;<sup>12,13</sup> however, the point-by-point scan mode limited the detection throughput. Bardin et al. presented an SPR spectro-imaging system introducing an additional spatial dimension.<sup>7</sup> This system is based on the illumination of a biochip through a vertical slit, and thus it can only be applied to analysis of linear multi-spot arrays due to the slit diffraction. We formerly reported a parallel scan wavelength-interrogation SPR imager which line-focused the light for signal excitation and was able to provide two-dimensional imaging of the whole array plane with a high throughput.<sup>11</sup> However, the sensing performance of this imager was in need of improvement.

Many efforts are currently devoted to the improvement of SPR sensing performance. It is well-known that SPR performance strongly depends on the quality of metal films, e.g., thickness and homogeneity. In theory, the minimum of SPR reflectivity can be zero, i.e., the contrast of SPR intensity profile can be infinity with an appropriate film thickness. However, the metal films can hardly satisfy optimum conditions due to the following reasons. Firstly, errors from the optimum thickness occur in the prepared metal films by magnetron sputtering or evaporation coating. Secondly, the biomolecular layer immobilized on the metal film can change the optimum thickness. Usually the properties of these biomolecules remain unknown, and thus the optimum film thickness can not be predicted

Address all correspondence to: Yonghong He, Tsinghua University, Graduate School at Shenzhen, Laboratory of Optical Imaging and Sensing, Shenzhen, 518055, China. Tel: +86-755-26036873; Fax: +86-755-26036395; E-mail: heyh@sz.tsinghua.edu.cn; Yanhong Ji, South China Normal University, MOE Key laboratory of Laser Life Science & Institute of Laser Life Science, Guangzhou, 510631, China. Tel: +86-20-85216052; Fax: +86-20-85216052; E-mail: jiyh@sncu.edu.cn.

theoretically. In order to overcome the above-mentioned problems, a phase-polarization contrast method called polarization interferometry (PI) has been proposed and applied to SPR biosensors.<sup>14</sup> PI techniques make use of the phase difference between two polarization components and enables one to lower the minimum of reflected intensity nearly to zero. Owing to the PI technique, films with non-optimum SPR coupling thicknesses can achieve good sensing performance, and the restrictions on allowable parameters of SPR-supporting metal films are reduced. At present, the PI technique has been experimentally realized in SPR systems with a monochromatic light source.<sup>10</sup> However, the realization of PI technique in wavelength-interrogation SPR sensors, which use white light as a source, still poses significant challenges because the critical optic of PI technique—the phase compensator—is extremely sensitive to wavelength.

In this work we design a new optic as the phase compensator which is based on the differences in the phase shift between *s*- and *p*- components when reflecting (*s*- or *p*- polarization means that the electric field of the light wave lies vertically to or just in the incidence plane, respectively). Different from conventional phase compensators, it is totally insensitive to wavelength. As a result, we successfully applied it to spectroscopic SPR systems and developed a PI based wavelength-interrogation SPR imager for analysis of microarrays. This paper is organized as follows: Firstly, the principle and experimental realization of PI techniques are presented. In particular, the optical design of this wavelength-insensitive phase compensator is discussed in detail. Secondly, system characterization of this PI based, parallel scan spectroscopic SPR imager was carried out. Detailed results are presented, including measurements of the refractive index resolution, the spatial resolving power, as well as the detection limit. Finally, a microarray experiment for identification of bacteria was conducted to demonstrate the biomedical application of this imager, and SPR results were further confirmed by fluorescence imaging.

## 2 Materials and Methods

### 2.1 Polarization Interferometry

Polarization interferometry (PI) technique exploits the phase difference between two polarization components to lower the minimum of the SPR dip and then increase the accuracy of the resonance-wavelength shift measurements.<sup>14</sup> Figure 1 shows the schematic of PI technique. Polarizer 1 is used to adjust the amplitude of *s*- and *p*- polarized components, in order that they have nearly the same amplitude when they pass through the SPR module. The phase compensator adjusts the phase difference between *s*- and *p*- components, in order that the resulting

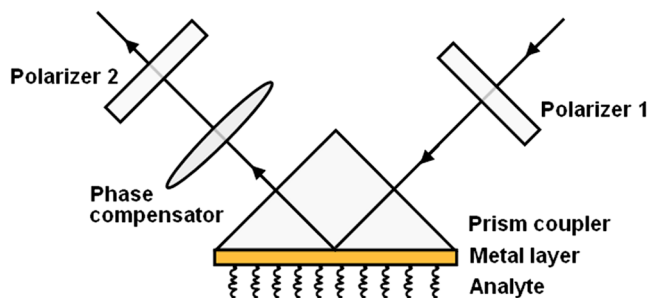


Fig. 1 Optical design of polarization interferometry.

reflected wave after the phase compensator is polarized linearly at the SPR minimum. The amplitude  $\mathbf{E}$  of the reflected wave is a vector sum of *s*- and *p*- polarized components. If polarizer 2 is placed perpendicular to  $\mathbf{E}$ , in theory, the exit intensity minimum would be zero, and the value of SPR contrast would be infinity. In actuality, the intensity minimum can hardly achieve zero exactly due to the non-idealities in the system.

Ordinarily, a quarter-wave plate is used as the phase compensator in an angle-interrogation SPR sensor which uses a single wavelength as the light source. However, as the quarter-wave plate is extremely sensitive to the wavelength, it can hardly be used for PI modulation in a wavelength-interrogation SPR system with a broadband light source. Figure 2 shows the phase difference between two polarization components passing through a 633 nm quarter-wave plate versus wavelength. It reveals that the phase difference value differs from 90 deg significantly if the wavelength deviates from 633 nm. The refractive index information used for drawing this plot is acquired from the research by Ghosh et al.<sup>15</sup> As far as we know, PI techniques have not yet been realized in a wavelength-interrogation SPR system as a result of wavelength dependence.

In this work, we propose a unique method of phase compensating which is insensitive to wavelength. Such a phase compensating method is based on the differences in the phase shift between *s*- and *p*- polarization components. If the light passes from dielectric 1 to dielectric 2 ( $n_1 > n_2$ ) at an angle equal to or larger than the angle of total reflection, the phase shifts of reflected *p*- and *s*- components can be expressed by Eqs. (1) and (2),

$$\delta_p = 2 \tan^{-1} \frac{n_1 [(n_1/n_2)^2 \sin^2 \theta - 1]^{1/2}}{n_2 \cos \theta}, \quad (1)$$

$$\delta_s = 2 \tan^{-1} \frac{n_2 [(n_2/n_1)^2 \sin^2 \theta - 1]^{1/2}}{n_1 \cos \theta}, \quad (2)$$

where  $n_1$  and  $n_2$  are refractive indices of dielectric 1 and dielectric 2, respectively, and  $\theta$  is the angle of incidence. According to the phase shifts, we designed and fabricated a rhombic prism for phase compensation, as shown in Fig. 3(a). It is demonstrated that the light beam undergoes two reflecting processes when it passes through this prism. In order that the rhombic prism can be used as a wavelength-insensitive quarter-wave compensator, the total difference  $\Delta$  which can be expressed as two times of  $|\delta_p - \delta_s|$ , should satisfy the following matching condition:

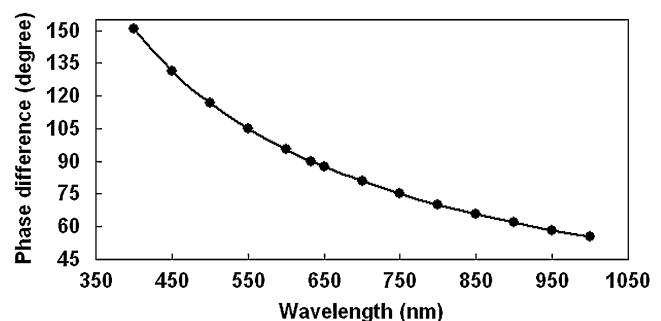
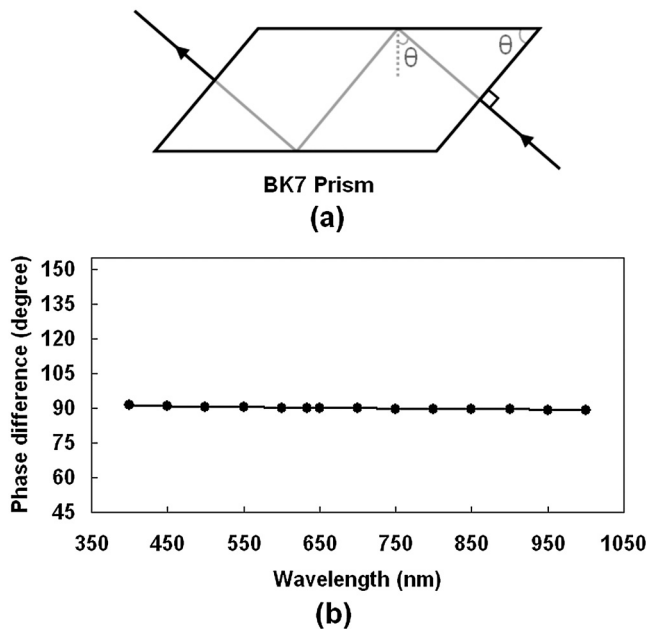


Fig. 2 Phase difference between two polarization components passing through a 633 nm quarter-wave plate versus wavelength.



**Fig. 3** Optical design and performance of the wavelength-insensitive rhombic prism. (a) Configuration of the prism. (b) Phase difference between two polarization components passing through the prism versus wavelength.

$$\Delta = 2|\delta_p - \delta_s| = \pi/2. \quad (3)$$

We choose BK7 glass as the material for fabrication of prism, whose refractive index is 1.51322 refractive index units (RIU) at 633 nm.<sup>15</sup> According to Eqs. (1), (2) and (3),  $\theta$  is calculated to be 55.05 deg. Then we investigate the wavelength dependence of this prism. As can be seen from Fig. 3(b), the phase difference varies slightly with the changing wavelength, revealing that the newly developed rhombic prism can be successfully applied to a wavelength-interrogation SPR system for phase compensation.

## 2.2 Imaging Systems Design

Figure 4 shows the schematic of the polarization interferometry based, parallel scan, wavelength interrogation SPR imager. As introduced in the last section, polarizer 1 in the incidence arm, and phase compensator as well as polarizer 2 in the emergence arm, form the main optics of PI technique. In this system, a halogen lamp with a power of 100 W is used as the light source.

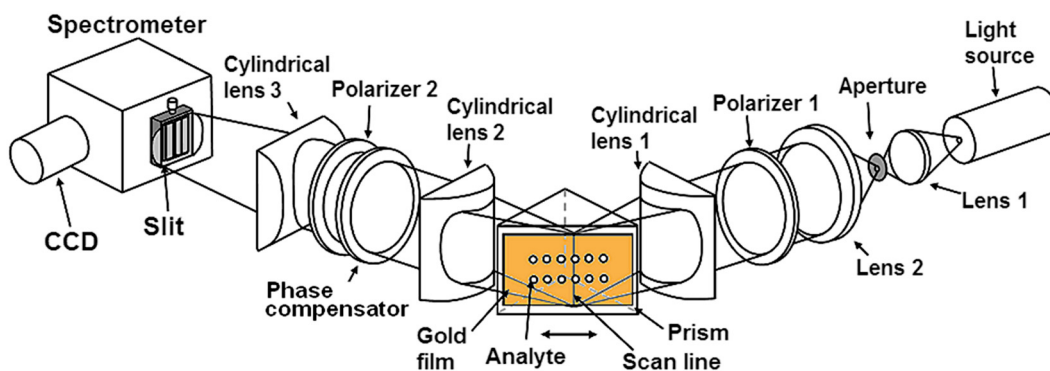


**Fig. 4** Schematic representation of this polarization interferometry based, wavelength-interrogation SPR imager.

The broadband light is focused by a 10× objective (lens 1) on an aperture and then collimated by lens 2. Then, cylindrical lens 1 focuses the light to a line on the surface of the microarray. In our system, the SPR module is configured in a Kretschmann manner with an attenuated total reflection method: a gold film is placed on the surface of a BK7 prism using a droplet of refractive index matching liquid ( $n:1.5148 \sim 1.5152$  RIU) to avoid entrapment of air-bubbles. The sensing layer is the surface of the gold film, where arrays of genetic elements are printed. The prism is fixed on a translation stage that enables a one-dimensional parallel scan. In the emergence arm, the reflected light beam is collimated by cylindrical lens 2. Then cylindrical lens 3 is placed to image the pattern of the sample, irradiated by the focused line light, to the entrance slit of a spectrometer. A charge coupled device (CCD) camera records the spectrally resolved images for further data analysis.

## 2.3 Fabrication of Microarrays

For the fabrication of DNA arrays, the magnetron sputtering gold films with a thickness of approximately 45 nm are used as substrates. The gold film needs to be cleaned thoroughly before the printing of sample spots. Firstly, the gold film is cleaned with a solution consisting of H<sub>2</sub>O<sub>2</sub> (30%), NH<sub>3</sub> (30%), and deionized water in a 1:1:5 ratio for 10 min.<sup>16</sup> Then, the film is dipped into acetone and ethanol for 10 min oscillating successively. After that, the film is thoroughly rinsed by deionized water and then dried for array printing.

Throughout this study, we print DNA-probe arrays manually. The DNA strands were thiolated for covalent bonding to gold films. After the printing process, the prepared array-chip, kept in a wet box, was then put into the electric heating constant temperature incubator (Shanghai Permanent Science and Technology the Limited Company, DHP-9052) for 2 h immobilization at 37 °C. Then, the chip was rinsed with deionized water to remove unbound DNA strands. The DNA-probe arrays can be used for system characterization or further hybridization with target genes for biomedical applications.

## 2.4 Spectral Data Analysis

Figure 5(a) shows an SPR sensing model with two spots of DNA strands printed on the substrate. Figure 5(b) is one of spectrally resolved images, corresponding to a certain position during optical scan. In this image, each row represents the SPR spectrum of one point on the irradiated line region. As can be seen, there is a certain pixel with minimum intensity in each row, corresponding

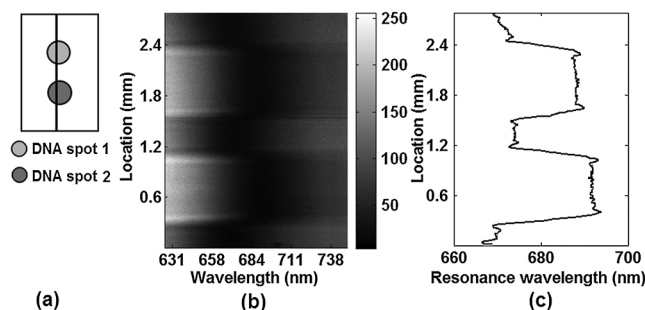


**Fig. 5** Spectral data analysis. (a) Design of the array. (b) One of dispersed images corresponding to a certain line region. (c) Distributions of the resonance wavelength of the scanned line region.

to the resonance wavelength when SPR occurs. In this way, we acquire the resonance wavelength of every point in this illuminated line region, as shown in Fig. 5(c). By analysis of all the images acquired during parallel scan, the distribution of resonance wavelengths of the whole array can be obtained. According to the relationship between the resonance wavelength and the refractive index, finally the array plane can be characterized by different refractive indices. In this way, the detection signals of the whole array plane, in terms of refractive index, are acquired for further biomedical analysis.

## 2.5 Fluorescence Imaging

In order to validate the biomolecular interactions on microarrays, the array chip is carefully removed from the SPR module and placed on the scan stage of a fluorescence imaging system after completion of the SPR experiment.<sup>17</sup> We have previously developed a quasi-confocal, hyperspectral fluorescence imaging system which provides accurate analysis of fluorescence-labeled microarrays.<sup>18</sup> The SPR and fluorescence results are compared and discussed.

## 3 System Characterization

### 3.1 Results of PI Modulation

Figure 6(a) shows a comparison of SPR curves without (curve 1) and with (curve 2) PI modulation. We acquire these SPR curves, detecting air around the sensing plane, with a piece of magnetron-sputtering gold film with a thickness of 38 nm. The film thickness is a little different from the optimized thickness of

approximately 45 nm when detecting air. We choose 38 nm for illustration here because in practice it is difficult to pre-set the film thickness at the optimum, due to complicated experimental conditions and difficulties of precise film-coating process control. As can be seen from Fig. 6(a), the minimum intensity decreases significantly as a result of PI modulation. The marked area is enlarged, as shown in the inset of Fig. 6(a). It is revealed from the inset that the noise fluctuation is also reduced by use of the PI technique. That is because the photon noise of the CCD camera is reduced with the decreasing of the incident intensity.

It is also demonstrated from Fig. 6(a) that there is a wavelength shift of the intensity minima from without PI to with PI, which results from the non-idealities of PI-comprising optics.<sup>14</sup> However, the phenomenon of wavelength shift after PI applies to all the points of the sensing plane. Strictly speaking, the relative shift of the resonance wavelength, not the absolute wavelength value, makes sense in the wavelength-interrogation SPR detection. If we choose a certain sample (such as air or water) as the refractive index reference, the absolute value of refractive index would not be affected. As a result of PI modulation, the restrictions on allowable parameters of SPR-supporting metal films and biomolecular layers are reduced.

The effect of the PI technique is also shown in the scanning image of an array-chip. The SPR images of  $2 \times 5$  DNA-probe arrays without and with PI modulation are shown in Figs. 6(b) and 6(c), respectively. By comparing these two images, it is revealed that the image quality of SPR results has been improved as a result of PI modulation, although the improvement observed from these two images is not quite obvious. Sometimes the concentration of analyte could be very low in real samples, and therefore a slight improvement in signal-to-noise ratio could make a significant difference.<sup>19,20</sup> The noise in the SPR system limits how small a change in refractive index can be reliably distinguished.<sup>20</sup> By employing the PI technique, the noise is efficiently suppressed, and the signal-to-noise ratio is enhanced as a result,<sup>21</sup> providing the potential of SPR biosensors for detecting analytes with extremely low concentrations.<sup>20,22</sup>

### 3.2 Refractive Index Resolution

The calculation of refractive index resolution is shown in Eq. (4),<sup>23</sup>

$$\delta n = \sigma / S_n, \quad (4)$$

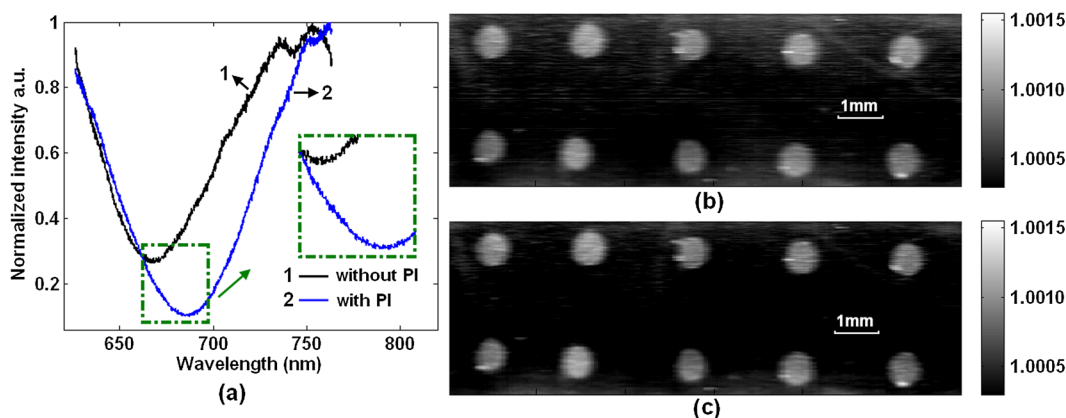


**Fig. 6** A comparison of SPR results without and with the modulation of polarization interferometry. (a) A comparison of SPR curves. (b) SPR image without polarization interferometry. (c) SPR image with polarization interferometry.

where  $\delta n$  is refractive index resolution,  $\sigma$  is standard deviation of SPR signal and  $S_n$  is the sensitivity of the system. For a wavelength-interrogation SPR system, sensitivity represents the relationship between the resonance wavelength and refractive index. The experiment will be carried out in the atmospheric environment, and thus we tested the sensitivity with the bare gold film naked in air. We changed the pressure of air around the SPR module step by step, so that refractive index of air varied with the changing pressure. Then we recorded the change of resonance wavelength that corresponds to the varying refractive index. The experimental results are shown in Fig. 7(a), and a sensitivity of  $1.03 \times 10^4$  nm/RIU is acquired. Then, we tested standard deviation  $\sigma$  of this wavelength-interrogation SPR system by detecting the resonance-wavelength fluctuations of air around the gold film. In order to make a comparison of sensing performance without and with PI modulation, both

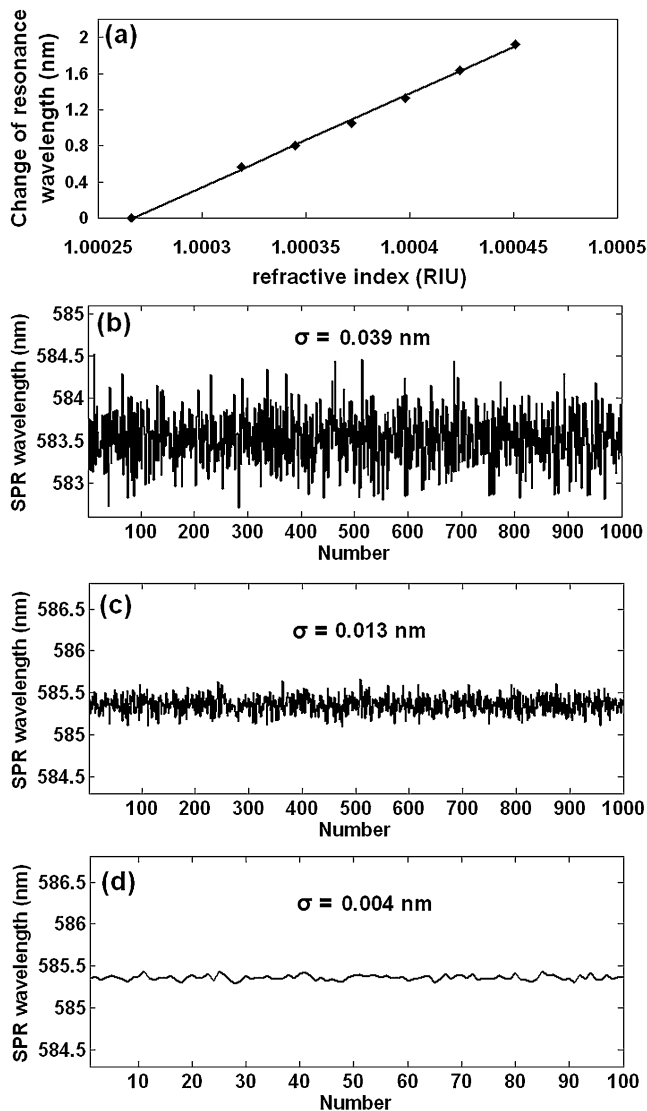


**Fig. 7** The refractive index resolution of this imager. (a) The relationship between the resonance wavelength and refractive index. (b) SPR wavelength fluctuations acquired without polarization interferometry. (c) SPR wavelength fluctuations acquired with polarization interferometry. (d) Fluctuations of the same data in (c) with neighboring 10 images averaged.

results are obtained, as shown in Figs. 7(b) and 7(c). The pressure, temperature, and humidity of air were maintained throughout the detection period. The experimental results demonstrate that the standard deviation of the PI-based system is much lower than that of the same system without application of PI technique, revealing that the PI technique contributes to the improvement of sensing performance. To further reduce noise level, we applied an image averaging method to data analysis. For an ideally independent noise with normal statistical distribution, the average of  $n$  images results in a decrease in the standard deviation by a factor of  $\sqrt{n}$  (Ref. 9). Figure 7(d) shows the fluctuations, corresponding to the same data as shown in Fig. 7(c), with neighbored 10 images averaged, and a standard deviation of 0.004 nm is acquired. Typically, the acquisition time per image is 1 sec. By using the image averaging method, the reduction of noise is at the expense of acquisition time, and thus a reasonable averaging number should be chosen according to the detection demand. According to Eq. (4), refractive index resolutions of  $1.3 \times 10^{-6}$  RIU under the normal condition and  $3.9 \times 10^{-7}$  RIU under this time-consuming condition are obtained from this system. The latter is comparable to the best reported in literature,<sup>5</sup> offering this system enormous potential for sensitive and accurate analysis of microarrays.

### 3.3 Spatial Resolution and Detection Limit

To test the spatial resolution of this system, we prepared a piece of gold film with patterns of ultrathin lines using a laser marking machine. Figure 8 shows the SPR image of the sensing plane. The center-to-center spacings of these vertical lines are approximately  $75 \mu\text{m}$ , and that of these horizontal lines are approximately  $85 \mu\text{m}$ . All the lines in this image can be clearly resolved, indicating that the spatial resolution of our system is better than  $100 \mu\text{m}$ . The spot diameters and center-to-center spacings of typical microarrays are of the order of  $\sim 100 \mu\text{m}$ ; thus, the spatial resolving power of this system is adequate for microarray analysis.

In SPR sensing, the detection limit is always demonstrated by detecting bacterial cells. Here the bacteria used are *Escherichia coli* DH-5 $\alpha$ . The gold coated substrates are firstly immersed in a solution of 16-mercaptohexadecanoic acid (1 mM) for 12 h for the obtaining of a dense self-assembled monolayer. The terminal carboxylic group is activated by EDC (1-ethyl-3-(3-dimethylaminopropyl) carbodiimide hydrochloride)/NHS (N-Hydroxysuccinimide) chemistry. The substrate was immersed in a solution of 0.4 mM EDC-0.1 mM NHS in reaction buffer (2- (N-morpholino) ethanesulfonic

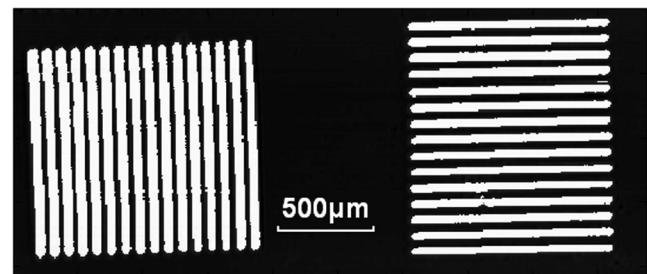


**Fig. 8** The spatial resolution of this imager. Center-to-center line spacing is  $75 \mu\text{m}$  for the vertical lines (left) and  $85 \mu\text{m}$  for the horizontal ones (right).

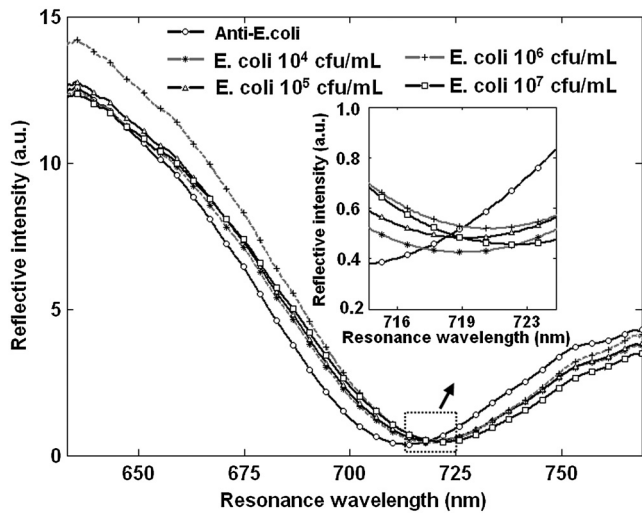


**Fig. 9** SPR curves corresponding to immobilized antibody and different concentrations of *Escherichia coli* for determining the detection limit of this imager.

acid 20.62 g/L, NaCl 29.2 g/L) for 30 min, and then a solution of 10  $\mu\text{g/ml}$  of anti-*E. coli* DH-5 $\alpha$  antibody was incubated over the substrate surface for 1 h. The non-specific sites were blocked by incubation with 0.1% bovine serum albumin (BSA) for 40 min. Then different concentrations of diluted *E. coli* DH-5 $\alpha$ , ranging from  $10^4$ – $10^7$  cfu/mL (colony-forming units per milliliter), were successively dropped onto the surface, and the detection results are shown in Fig. 9. Furthermore, these curves near the resonance wavelength are enlarged and shown in the inset. The resonance wavelengths corresponding to the solutions of diluted *E. coli* DH-5 $\alpha$  ( $10^4$ – $10^7$  cfu/mL) were 719.0, 719.5, 720.3, and 721.7 nm, respectively. The experimental data reveal that the increase of *E. coli* concentration leads to that of resonance wavelength, which could be attributed to the specific recognition of bacteria with the antibody. We acquire a detection limit of  $10^4$  cfu/mL with a good repeatability, which is comparable to the reported values in the literature.<sup>24–26</sup>

#### 4 Biomedical Application of Microarrays

The identification of bacteria by imaging gene chips is performed by this spectroscopic SPR imager as an example of biomedical applications of microarrays. In order to confirm the SPR results, these array-chips are imaged by a fluorescence imaging system after completion of SPR experiments. The complementary target genes were labeled with fluorescent dyes, in order that the hybridized arrays can provide both SPR and fluorescence signals. Throughout this study, Cy5 (absorption/emission: 649/667 nm) and Dylight 680 (absorption/emission: 680/715 nm) were used as fluorescent labels. Both the DNA probes and fluorescence-labeled target genes are purchased from TaKaRa Biotechnology (Dalian, China).

In this experiment, the DNA fragments were labeled with fluorophores to validate SPR results. Therefore, we carried out a test before this experiment to investigate whether fluorophores affect SPR results. We prepare an array-chip with 6 spots of DNA probes with the same concentration of 0.1  $\mu\text{mol/L}$ . The left 3 spots are label-free, while the other 3 spots are labeled with Cy5. The SPR results are shown in Fig. 10(a), and the refractive index graph of the marked row in Fig. 10(a) is shown in Fig. 10(b). As can be seen, the values of refractive index of these 6 spots are nearly identical. Figure 10(c) shows the corresponding fluorescent images. Our experiment with Dylight 680 shows similar results (data not shown). These imaging results demonstrate that the labeled fluorophores have little influence in the SPR results, providing the potential for subsequent validation experiments.

Then we carried out the experiment of DNA hybridization. The gold-film-covered quartz is used as the substrate, where four  $4 \times 5$  probe arrays were printed manually. As shown in Fig. 11(a), the array comprises one row of  $\beta$ -hemolytic streptococcus probes [5'(SH)-T18ACCGTCACTTGGTGGATT-3'] with a concentration of 2  $\mu\text{M}$ , one row of *Escherichia coli* probes [5'(SH)-T18ACGGTTACCTTGTACGACTT-3'] with a concentration of 2  $\mu\text{M}$ , one row of non-specific DNA sequence as negative control (5'(SH)-T18AGAAGCAAGC TTCTCGTCCG-3') which can be served as quality report marks of the chip hybridization, and one row of positive

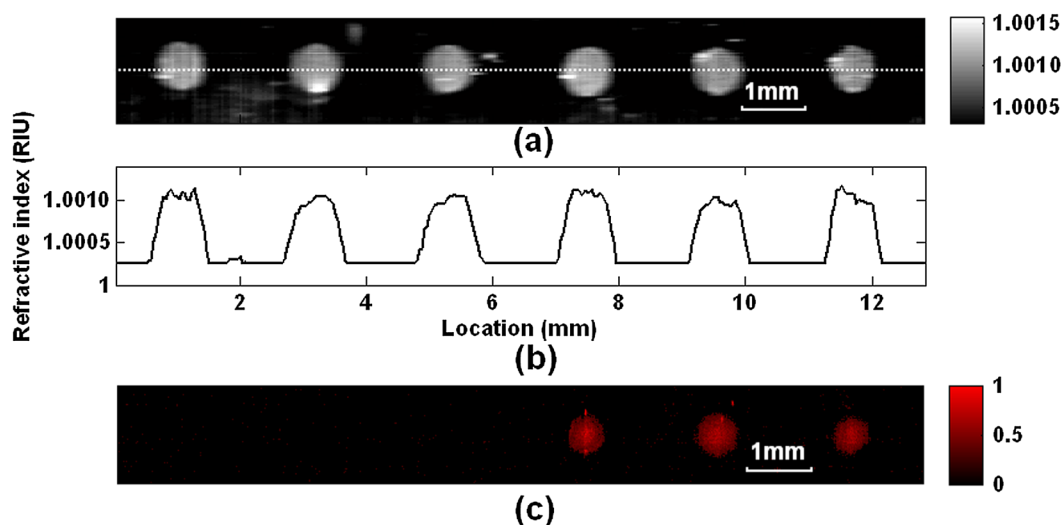


**Fig. 10** SPR and fluorescent results with both label-free spots (left 3) and spots labeled with Cy5 (right 3). (a) SPR image of the array-chip. (b) Refractive index graph of the marked row in (a). (c) Corresponding fluorescent image of the array-chip.

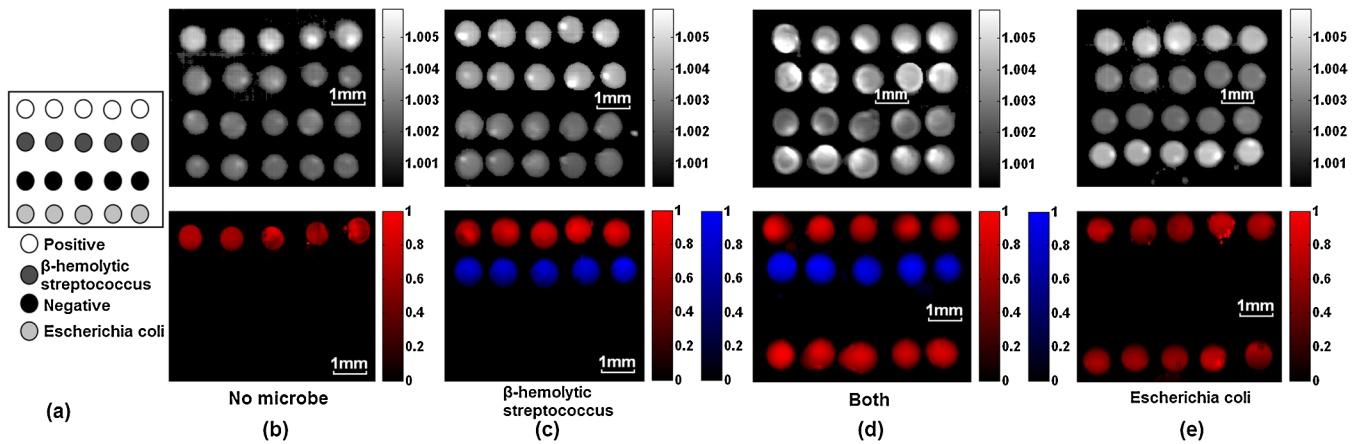


**Fig. 11** Identification of bacteria as an example of biomedical applications of microarrays. (a) Design of the array. Scanning results with (b) no microbe, (c) only *β-hemolytic streptococcus*, (d) both two microbes, and (e) only *Escherichia coli* DNA fragments in the sample solution. The top images show SPR results, and the bottom images show fluorescence results as confirmations of SPR results.

probes [fluorescence labeled probe DNA strands: [5'(SH)-T18AGAGTTTGCCTGGCTCAG-3'(Cy5)] with a concentration of 5  $\mu$ M. The repetition of the same 5 spots in each row is used to demonstrate the credibility of the experiment.

Then the probe arrays were hybridized with different kinds of sample solutions, and imaged by SPR and fluorescence systems, respectively. The top images in Figs. 11(b)–11(e) show the SPR results. Figure 11(b) shows the detection results with no microbe DNA fragments present in the sample solution. As expected, only the positive probes report a high signal. If the complementary *Escherichia coli* DNA sequence is present in a sample, then the row of *Escherichia coli* probes will show a high signal. Similarly, the row of *β-hemolytic streptococcus* probes will show a high signal if *β-hemolytic streptococcus* is present in the sample. As can be seen from Figs. 11(c) and 11(e), the SPR results correspond well with expectation. Figure 11(d) shows the results with both *Escherichia coli* and *β-hemolytic streptococcus* in the sample, and then all the rows of probes, except the row of negative probes, show a high signal.

After acquisition of SPR results, these arrays were carefully removed to the scan stage of a fluorescence imaging system. Fluorescence signals of these arrays were acquired to confirm SPR results. Fluorescent dye of Cy5 was labeled to positive and *Escherichia coli* DNA fragments, and Dylight 680 was used for *β-hemolytic streptococcus*. Colors of red and blue represent different dyes. The bottom images in Figs. 11(b)–11(e) show the fluorescence imaging results. As expected, a certain row of probes will show a high fluorescent intensity signal if the corresponding microbe DNA fragments are present in the sample, otherwise these rows will show a low (or zero) signal, revealing that the target genes are selectively hybridized to the chip-bound probes. As can be seen from these images, fluorescence results correspond well with SPR results, indicating that the proposed SPR imager can be successfully applied to biomedical research.

## 5 Conclusions

In this work, we have proposed a polarization-interferometry-based, wavelength-interrogation SPR imager. By developing a wavelength-insensitive rhombic prism as the phase compensator, we successfully apply a PI technique to a wavelength-interrogation SPR system. As a result of PI modulation, combined with the use of a fit algorithm, the sensing

performance is greatly improved. A refractive index resolution of  $1.3 \times 10^{-6}$  RIU is acquired under the normal condition, and an improved resolution of  $3.9 \times 10^{-7}$  RIU is obtained with neighboring 10 images averaged. Such a resolution achieves the best performance level of SPR sensors using conventional surface plasmons. This system employs a pushbroom scan architecture that line-focuses the excitation light on the array plane, and records the complete SPR curve for every voxel of the plane by parallel scan of the line light. In this way, the detection throughput is greatly improved compared with monochannel SPR sensing systems, making this imager particularly suitable for analysis of microarrays. A spatial resolution better than 100  $\mu$ m and a detection limit of  $10^4$  cfu/mL of *Escherichia coli* bacteria were acquired from this system, which is adequate for microarray detection. The application of this SPR system is demonstrated by reading microarrays for identification of bacteria, and the SPR results are in accordance with the fluorescence results. We believe that the proposed polarization interferometry based SPR imager could be used to build a commercially valuable instrument for biomedical research.

## Acknowledgments

This research was made possible with the financial support from NSFC China (grants 81171375), Program for New Century Excellent Talents in University and Shenzhen Science Fund for Distinguished Young Scholars (2010).

## References

1. S. P. A. Fodor et al., "Light-directed, spatially addressable parallel chemical synthesis," *Science* **251**(4995), 767–773 (1991).
2. P. O. Brown and D. Botstein, "Exploring the new world of the genome with DNA microarrays," *Nat. Genet.* **21**(suppl: S), 33–37 (1999).
3. J. Homola, "Present and future of surface plasmon resonance biosensors," *Anal. Bioanal. Chem.* **377**(3), 528–539 (2003).
4. J. Homola, "Surface plasmon resonance sensors for detection of chemical and biological species," *Chem. Rev.* **108**(2), 462–493 (2008).
5. M. Piliarik and J. Homola, "Surface plasmon resonance (SPR) sensors: approaching their limits?," *Opt. Express* **17**(19), 16505–16517 (2009).
6. B. Rothenhausler and W. Knoll, "Surface-plasmon microscopy," *Nature* **332**(6165), 615–617 (1988).
7. F. Bardin et al., "Surface plasmon resonance spectro-imaging sensor for biomolecular surface interaction characterization," *Biosens. Bioelectron.* **24**(7), 2100–2105 (2009).

8. S. J. Chen et al., "Surface plasmon resonance phase-shift interferometry: real-time DNA microarray hybridization analysis," *J. Biomed. Opt.* **10**(3), 034005 (2005).
9. L. Liu et al., "Detection of methane by a surface plasmon resonance sensor based on polarization interferometry and angle modulation," *Opt. Lasers Eng.* **48**(12), 1182–1185 (2010).
10. L. Liu et al., "A two-dimensional polarization interferometry based parallel scan angular surface plasmon resonance biosensor," *Rev. Sci. Instrum.* **82**(2), 023109 (2011).
11. L. Liu et al., "Parallel scan spectral surface plasmon resonance imaging," *Appl. Opt.* **47**(30), 5616–5621 (2008).
12. J. S. Yuk et al., "Analysis of protein interactions on protein arrays by a wavelength interrogation-based surface plasmon resonance biosensor," *Proteomics* **4**(11), 3468–3476 (2004).
13. J. W. Jung et al., "High-throughput analysis of GST-fusion protein expression and activity-dependent protein interactions on GST-fusion protein arrays with a spectral surface plasmon resonance biosensor," *Proteomics* **6**(4), 1110–1120 (2006).
14. A. V. Kabashin et al., "Phase-polarisation contrast for surface plasmon resonance biosensors," *Biosens. Bioelectron.* **13**(12), 1263–1269 (1998).
15. G. Ghosh, "Dispersion-equation coefficients for the refractive index and birefringence of calcite and quartz crystals," *Opt. Commun.* **163**(1–3), 95–102 (1999).
16. R. H. Wang et al., "Immobilisation of DNA probes for the development of SPR-based sensing," *Biosens. Bioelectron.* **20**(5), 967–974 (2004).
17. J. B. Beusink et al., "Angle-scanning SPR imaging for detection of biomolecular interactions on microarrays," *Biosens. Bioelectron.* **23**(6), 839–844 (2008).
18. Z. Liu et al., "Quasi-confocal, multichannel parallel scan hyperspectral fluorescence imaging method optimized for analysis of multicolor microarrays," *Anal. Chem.* **82**(18), 7752–7757 (2010).
19. T. Vo-Dinh and B. Cullum, "Biosensors and biochips: advances in biological and medical diagnostics," *Fresenius J. Anal. Chem.* **366**(6–7), 540–551 (2000).
20. X. Wang et al., "Shot-noise limited detection for surface plasmon sensing," *Opt. Express* **19**(1), 107–117 (2011).
21. Z. Sun, Y. He, and J. Guo, "Surface plasmon resonance sensor based on polarization interferometry and angle modulation," *Appl. Opt.* **45**(13), 3071–3076 (2006).
22. T. M. Davis and W. D. Wilson, "Determination of the refractive index increments of small molecules for correction of surface plasmon resonance data," *Anal. Biochem.* **284**(2), 348–353 (2000).
23. J. Homola, S. S. Yee, and G. Gauglitz, "Surface plasmon resonance sensors: review," *Sens. Actuators, B* **54**(1–2), 3–15 (1999).
24. H. Baccar et al., "Surface plasmon resonance immunosensor for bacteria detection," *Talanta* **82**(2), 810–814 (2010).
25. Y. Wang et al., "Subtractive inhibition assay for the detection of E. coli O157:H7 using surface plasmon resonance," *Sensors* **11**(3), 2728–2739 (2011).
26. Z. Liu et al., "Parallel-scan based microarray imager capable of simultaneous surface plasmon resonance and hyperspectral fluorescence imaging," *Biosens. Bioelectron.* **30**(1), 180–187 (2011).